

Acoustic Frequency Multiplication and Pure Second Harmonic Generation of Phonons by Magnetic Transducers

Chengyuan Cai,^{1,*} Xi-Han Zhou,^{1,*} Weichao Yu,^{2,3} and Tao Yu^{1,†}

¹*School of Physics, Huazhong University of Science and Technology, Wuhan 430074, China*

²*State Key Laboratory of Surface Physics and Institute for Nanoelectronic*

Devices and Quantum Computing, Fudan University, Shanghai 200433, China

³*Zhangjiang Fudan International Innovation Center, Fudan University, Shanghai 201210, China*

(Dated: December 8, 2022)

We predict frequency multiplication of surface acoustic waves in dielectric substrates via the ferromagnetic resonance of adjacent magnetic transducers when driven by microwaves. We find *pure* second harmonic generation (SHG) without any linear and third harmonic components by a magnetic nanowire. The SHG and linear phonon pumping are switched by varying the saturated magnetization direction of the wire, or resolved directionally when pumped by magnetic nano-disc. We address the high efficiency of SHG with comparable magnitude to that of linear response, as well as unique non-reciprocal phonon transport that is remarkably distinct in different phonon harmonics. Such acoustic frequency comb driven by microwaves should bring unprecedented tunability for the miniaturized phononic and spintronic devices.

Introduction.—Surface acoustic waves (SAWs) are important information carriers in phononic and electronic devices [1, 2], but also act as excellent information mediators for quantum communication in high-quality piezoelectric substrates [3–5]. Downscaled phononic devices rely on the generation of coherent phonons of above GHz frequency and sub-micrometer wavelength, which arguably represents one challenge by conventional electric approach so far since its excitation efficiency is low and energy consumption is high [6–8]. In contrast, the ferromagnetic resonance (FMR) of magnetic nanostructures can pump such phonons via the magnetostriction efficiently in conventional dielectric substrates [9–19], which achieves efficient communication of spin information over millimeter distance. The inverse process, i.e., the modulated transmission of SAWs via magnetostriction, was verified decades ago in a magnetoelastic bilayer towards SAW isolator functionality [20], but recently obtains tremendous attention due to its remarkable non-reciprocity or diode effect with large on-off ratios observed in many ferromagnet/piezoelectric insulator heterostructures [21–27]. Most of these studies focus on the linear response, however, a regime limiting the tunability and maximal frequency of resonant phonons.

High phonon harmonics in the acoustic frequency multiplication, or the acoustic frequency comb, operate at a higher frequency and shorter wavelength than their linear component [28–31]. In crystals their coherent generation relies on the anharmonic interaction of lattice and thus needs to exploit strong laser fields to achieve the demanding nonlinearity that may cause unavoidable parasitic effects such as heating and dephasing. Second harmonic generation (SHG) of phonons in the terahertz frequency was excited in ultrashort time scales [28, 29], where strong laser pulses are exerted, as well as in the megahertz frequency for the ultrasonic waves [30]. Without piezoelectricity [31], achieving such nonlinearity for

GHz phonons appears to be a formidable task. Different from the electric approach, nonlinear magnetization dynamics for frequency multiplication is easily accessible, energy-saving, and well controlled by microwaves [32–37].

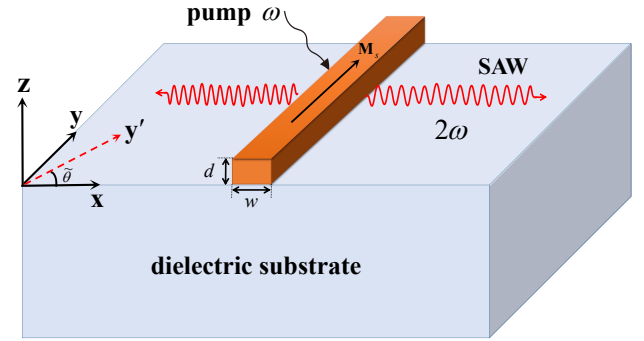


Figure 1. Pure SHG 2ω of SAWs in conventional dielectric substrates via phonon pumping by the FMR of a magnetic nanowire of thickness d and width w that is launched by microwaves of frequency ω . The saturated magnetization M_s is biased by an external magnetic field, allowing the pure second harmonics of SAWs to mix with other components when away from the wire direction.

In this Letter, we predict the acoustic frequency multiplication as well as *pure* SHG of SAWs of ~ 10 GHz frequency in conventional non-piezoelectric dielectric substrates, in which the linear and third harmonic harmonics completely vanish, via the phonon pumping of adjacent magnetic transducers that are launched by microwaves, as sketched in Fig. 1 for the magnetic nanowire configuration (such a wire is later replaced by a magnetic nano-disc). We can switch the pure SHG, when the saturated magnetization is along the wire direction, to the dominant linear phonon excitation, when the magnetization is biased to the wire normal direction, or realize their mixing flexibly with other arbitrary magnetization

directions. All such phenomena can be exhibited conveniently with an in-plane magnetized nano-disc, where the pure SHG and linear response are resolved directionally. We find the efficiency of such SHG is high since with accessible magnetization nonlinearity its magnitude is not smaller than that of linear response, but the non-reciprocity appearing in the linear phonon pumping is strongly altered in the SHG due to the distinct dynamic magnetoelastic boundary conditions.

Model and acoustic frequency multiplication.—The magnetoelastic heterostructure that we consider contains a nano-magnet “M” of thickness d with an in-plane equilibrium magnetization \mathbf{M}_s , such as a magnetic nanowire of width w or a magnetic nano-disc of radius r , and an adjacent thick dielectric substrate “N”, which couple via the magnetostriction [11, 15, 17, 25, 38, 39]

$$F_{\text{me}} = \frac{1}{M_s^2} \int d\mathbf{r} \left(B_{||} \sum_i \varepsilon_{ii} M_i^2 + B_{\perp} \sum_{i \neq j} \varepsilon_{ij} M_i M_j \right),$$

where $B_{||}$ and B_{\perp} are the magneto-elastic coupling constants, $\{i, j\} = \{x, y, z\}$ denote the spatial index, and $\varepsilon_{ij} \equiv (1/2) (\partial u_i / \partial r_j + \partial u_j / \partial r_i)$ is the strain tensor defined via the displacement field \mathbf{u} . Here we focus on the FMR of the nano-magnet [13, 18], such that the precessing magnetization $\mathbf{M}(t)$ can be treated as a macrospin, which is governed by the Landau-Lifshitz-Gilbert (LLG) equation [40, 41]:

$$\partial \mathbf{M} / \partial t = -\mu_0 \gamma \mathbf{M} \times \mathbf{H}_{\text{eff}} + \alpha (\mathbf{M} / M_s) \times \partial \mathbf{M} / \partial t, \quad (1)$$

where μ_0 is the vacuum permeability, $-\gamma$ is the electron gyromagnetic ratio, and α is the phenomenological damping constant [40]. The magnetization precesses around an effective magnetic field $\mathbf{H}_{\text{eff}} = \mathbf{H}_{\text{app}} + \mathbf{H}_d + \mathbf{H}_{\text{ex}} + \mathbf{H}_e$ that contains the external field \mathbf{H}_{app} including the static \mathbf{H}_0 and dynamic $\mathbf{h}(t)$ fields, the demagnetizing field $\mathbf{H}_d = (-N_{xx}M_x, -N_{yy}M_y, -N_{zz}M_z)$, where $N_{xx} \simeq d/(d+w)$, $N_{yy} \simeq 0$, and $N_{zz} \simeq w/(d+w)$ parameterize the demagnetization factor of the wire [42], the exchange field $\mathbf{H}_{\text{ex}} = A_{\text{ex}} \nabla^2 \mathbf{M}$ with the exchange stiffness A_{ex} , as well as the effective field due to the magnetostriction

$$\begin{aligned} H_{e,i} &\equiv -(1/\mu_0) \delta F_{\text{me}} / \delta M_i(\mathbf{r}) \\ &= -\frac{2}{\mu_0 M_s} \sum_j \varepsilon_{ij} M_j \left[\delta_{ij} B_{||} + (1 - \delta_{ij}) B_{\perp} \right]. \end{aligned} \quad (2)$$

As a backaction, the magnetization also affects the static and dynamic strains of the elastic heterostructure. We have to distinguish the displacement fields in the nano-magnet $\mathbf{u}_M(\mathbf{r}, t)$ and the dielectric substrate $\mathbf{u}_N(\mathbf{r}, t)$, as well as their different material densities ρ_M and ρ_N in the elastic equations of motion [16, 43–45]:

$$\begin{aligned} \rho_M \ddot{\mathbf{u}}_M &= \nabla \cdot (\vec{\sigma}_M + \vec{\eta}), \\ \rho_N \ddot{\mathbf{u}}_N &= \nabla \cdot \vec{\sigma}_N, \end{aligned} \quad (3)$$

which are governed by the mechanical stress tensor

$$\sigma_{ij}^{N,M} = \delta_{ij} \lambda_{N,M} \sum_l \varepsilon_{ll}^{N,M} + 2\mu_{N,M} \varepsilon_{ij}^{N,M}, \quad (4)$$

where $\lambda_{N,M}$ and $\mu_{N,M}$ are the associated Lamé constants, and the magnetization stress tensor inside the magnet

$$\begin{aligned} \eta_{ij} &\equiv \partial F_{\text{me}} / \partial (\partial u_i / \partial r_j) \\ &= M_i M_j [\delta_{ij} B_{||} + (1 - \delta_{ij}) B_{\perp}] / M_s^2. \end{aligned} \quad (5)$$

However, with uniform magnetization there is no net effect of $\vec{\eta}$ inside the magnet since $\nabla \cdot \vec{\eta} = 0$. All the phonon pumping effect thereby comes from the static and dynamic magnetization stress at the boundary of the magnet, which appears in the boundary conditions defined by the continuity of the force per unit area or the stress vector at the surfaces and interfaces [16, 17, 43–45]:

$$\begin{aligned} \vec{\sigma}_N \cdot \mathbf{n}|_A &= 0, \\ (\vec{\sigma}_M + \vec{\eta}) \cdot \mathbf{n}|_B &= 0, \\ (\vec{\sigma}_M + \vec{\eta}) \cdot \mathbf{n}|_C &= \vec{\sigma}_N \cdot \mathbf{n}|_C. \end{aligned} \quad (6)$$

Here we denote the interfaces between the dielectric substrate and vacuum as “A”, between the nano-magnet and vacuum as “B”, and between the dielectric substrate and nano-magnet as “C”, such that \mathbf{n} is the normal unit vector of each interface.

When \mathbf{M}_s is aligned to the wire $\hat{\mathbf{y}}$ -direction, the dynamic boundary magnetization stress in the linear order of fluctuated magnetization $\vec{\eta} \cdot \mathbf{n}|_C = M_z B_{\perp} / M_s \hat{\mathbf{y}}$ is along the wire direction, as well as $(\vec{\eta} \cdot \mathbf{n}|_B) \parallel \hat{\mathbf{y}}$, which thereby excites no SAW propagating *normal* to the wire direction since its associated mechanical stress vector along the wire direction vanishes and thereby mismatches. We thereby expect the absence of linear harmonics for the pumped SAWs propagating normally to the wire in such a magnetic configuration.

We substantiate such expectation by numerical simulations, but allow an arbitrary in-plane saturated magnetization by an angle θ with respect to the wire normal $\hat{\mathbf{x}}$ -direction (Fig. 1), which we find is nearly parallel to the external static field \mathbf{H}_0 [46]. We combine the LLG equation (1) with the elastic equations of motion (3) under the boundary conditions (6) in COMSOL Multiphysics [47, 48]. We choose the nano-magnet as the yttrium iron garnet (YIG) nanowire [49] of thickness $d = 80$ nm, width $w = 150$ nm, and saturated magnetization $\mu_0 M_s = 0.177$ T [13, 18], biased by $\mu_0 H_0 = 0.1$ T, which has high magnetic quality with $\alpha = 10^{-4}$. It is adjacent to a thick gadolinium gallium garnet (GGG) substrate that has high acoustic quality [13, 18]. Their elastic properties are close but not identical: for YIG, $\rho_M = 5170$ kg/m³, $\lambda_M = 1.16 \times 10^{11}$ N/m², $\mu_M = 7.64 \times 10^{10}$ N/m² [11], while for GGG, $\rho_N = 7080$ kg/m³, $\lambda_N = 1.27 \times 10^{11}$ N/m², $\mu_N = 8.83 \times 10^{10}$ N/m² [50]. They are coupled via magnetostriction with the coupling constants

$B_{||} = 3.48 \times 10^5 \text{ J/m}^3$ and $B_{\perp} = 6.96 \times 10^5 \text{ J/m}^3$ [11]. The sound velocity of SAWs $c_r = 3271.8 \text{ m/s}$ [51].

We apply an in-plane broadband magnetic field transverse to the saturated magnetization $\mathbf{h}(t) = h_0 \sin(\omega_F t) \hat{\mathbf{x}}'$ with a short duration time $0 \leq t \leq 2\pi/\omega_F$, where $\hat{\mathbf{x}}' \perp \mathbf{M}_s \perp \hat{\mathbf{z}}$, with which we adjust the FMR frequency $\omega_F/(2\pi) = \{5.43, 3.71, 2.29\} \text{ GHz}$ and the field strength $\mu_0 h_0 = \{9.05, 6.20, 3.83\} \text{ mT}$ to make sure the pumped transverse magnetization $M_{z'} \approx 0.15 M_s$ or the precession angle $\sim 8.5^\circ$.

Figure 2 plots the frequency multiplication of SAWs up to the third harmonic generation (THG) by the FMR of YIG nanowire with different magnetic configurations, characterized by the pumped displacement field u_z at the surface $z = 0$ (a-c), their Fourier components u_k (d-f), as well as the oscillation frequency and wave number resolved from the peaks in u_k in comparison to the SAW dispersion (g-i). The excellent agreement of the oscillation frequency and wave vector with the SAW dispersion $\omega_k = c_r |k|$ implies that the pumped elastic strain at the surface is dominated by SAWs. Static strains exist only near the nano-magnet but vanish when \mathbf{M}_s is along the wire direction because of the absence of static $\vec{\eta}$.

One remarkable feature in Fig. 2 is that when the saturated magnetization is along the wire direction ($\tilde{\theta} = \pi/2$), there is only the SHG of SAWs propagating normally to the wire, without any linear and third harmonics, while when \mathbf{M}_s is normal to the wire direction ($\tilde{\theta} = 0$), the linear response (LR) dominates. Such SHG comes completely from the nonlinearity of magnetic stress at the boundary, which scales as h_0^2 in its amplitude, thus distinguished from the anharmonicity effect of lattice [28, 29]. The mixing of SHG and other harmonics is realized when \mathbf{M}_s is away from the parallel setup, e.g., $\tilde{\theta} = \pi/4$ in Fig. 2(b,e,h). The THG is unique since it comes from the interaction between magnons but not the nonlinear magnetic stress $\propto \exp(2i\omega_F t)$ [46]. These provide flexible tunability for the demanding phonon frequency achievable by different directions and magnitudes of the static magnetic field.

Pronounced non-reciprocity exists in the linear phonon pumping, as shown in Fig. 2(e) when $\tilde{\theta} = \pi/4$. Such non-reciprocity vanishes when the magnetization is normal to the wire direction as in Fig. 2(f). These numerical results agree with the theoretical expectations from the previous analytical solutions [15, 16]. However, in the SHG the non-reciprocity is generally suppressed in almost all the magnetic configurations, as shown by the Fourier components with opposite momenta in Fig. 2(d,e,f).

Quantum formalism.—Above simulated phonon high harmonic generation can best be formulated in a quantum language. The magnetization operators $\hat{M}_{x',z'} \simeq -\sqrt{2\gamma\hbar M_s}(\mathcal{M}_{x',z'} \hat{m} + \mathcal{M}_{x',z'}^* \hat{m}^\dagger) + \mathcal{O}(\hat{m}^3)$ and $\hat{M}_{y'} \simeq M_s - \gamma\hbar[\mathcal{M}_{z'}^2(\mathbf{r}) + \mathcal{M}_{x'}^2(\mathbf{r})] \hat{m}\hat{m} - \gamma\hbar[\mathcal{M}_{z'}^2(\mathbf{r}) + \mathcal{M}_{x'}^2(\mathbf{r})] \hat{m}^\dagger \hat{m}^\dagger + \mathcal{O}(\hat{m}^3)$ contain the linear

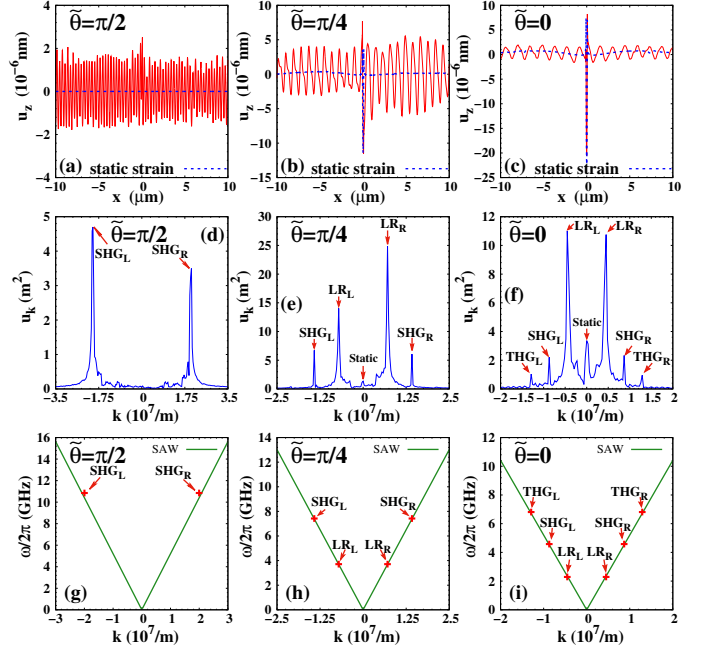


Figure 2. Acoustic frequency multiplication in GGG substrates by the FMR of adjacent YIG nanowire with different magnetic configurations, plotted about 10 ns after the end of magnetic-field pulse. The blue dashed lines in (a-c) indicate the static strain that is pronounced only near the nano-magnet. When \mathbf{M}_s is aligned to the wire direction with $\tilde{\theta} = \pi/2$, there is only the SHG in the pumped SAWs, as shown by the displacement field u_z at the surface $z = 0$ in (a), the resolved Fourier component u_k in (d), as well as the oscillation frequency and wave vector of u_z by crosses in comparison with the SAW dispersion in (g). In the other magnetic configurations with $\tilde{\theta} = \pi/4$ [(b), (e), (h)] and $\tilde{\theta} = 0$ [(c), (f), (i)], the LR, SHG, and THG coexist with flexible tunability by magnetization directions.

Holstein-Primakoff [52–57] expansion of Kittel magnon \hat{m} and their dominant interactions with strength governed by the ellipticity of eigenmodes $\mathcal{M}_{x'} = i\xi_m^2 \mathcal{M}_{z'}$ [46], which are not circularly polarized when the form factor $\xi_m \neq 1$. The eigenmodes $\mathbf{u}(x, z, k)$ of SAWs in the elastic heterostructure contain both near-field solution close to the magnet and far-field $|x| \gg w/2$ solution that converges asymptotically to those of SAWs [51]. In terms of them and the SAW operator \hat{p}_k , we quantize the displacement field

$$\hat{\mathbf{u}}(x, z, t) = \sum_k \left(\mathbf{u}(x, z, k) \hat{p}_k + \mathbf{u}^*(x, z, k) \hat{p}_k^\dagger \right). \quad (7)$$

Substituting into magnetostriction energy, we obtain the magnon-phonon coupling Hamiltonian $\hat{H}_c = \hbar \sum_{n \geq 1} \sum_k g_k^{(n)} (\hat{m}^\dagger)^n \hat{p}_k + \text{H.c.}$ (refer to the Supplementary Material [46] for details), where the n -th order coupling constants $g_k^{(n)}$ rely on the near-field solution of SAWs. $g_k^{(3)}$ vanishes for the circular precession $\xi_m = 1$, and when \mathbf{M}_s is parallel to the wire direction, $g_k^{(1)}$ and

$g_k^{(3)}$ vanish, leading to the pure SHG [46]. So the linear fluctuation of \hat{m} is responsible for the LR and SHG of SAWs, while the double frequency in \hat{m}^2 , existing in elliptical precessions $\xi_m \neq 1$, causes the THG. The interaction is “non-reciprocal” when $|g_k^{(n)}| \neq |g_{-k}^{(n)}|$.

Including broadband microwaves $\mathbf{h}(t) = h_{x'}(t)\hat{\mathbf{x}}'$ and the damping rates of magnons and phonons δ_m and δ_p , the magnon and surface phonon obey the Langevin's equations [58, 59]

$$\begin{aligned} d\hat{m}/dt &= -i(\omega_F - i\delta_m)\hat{m} - i \sum_{n \geq 1} \sum_k n g_k^{(n)} (\hat{m}^\dagger)^{(n-1)} \hat{p}_k \\ &\quad - \mu_0 \sqrt{\gamma M_s V / (2\hbar)} \xi_m h_{x'}(t), \\ d\hat{p}_k/dt &= -i(\omega_k - i\delta_p)\hat{p}_k - i \sum_{n \geq 1} g_k^{(n)*} \hat{m}^n, \end{aligned} \quad (8)$$

where $V = wdl$ is the wire's volume with length l . Here we focus on a large coherent pumping such that the magnon's thermal population is much smaller than that driven by microwaves. To solve the nonlinear Eq. (8), we apply the mean-field approximation $\hat{A}\hat{B} = \langle \hat{A} \rangle \hat{B} + \hat{A} \langle \hat{B} \rangle$ for operators. Below we denote the ensemble-averaged $\langle \hat{A} \rangle = A$. Disregarding the far-off-resonant excitation, we find in the frequency domain the coherent amplitudes of SAWs

$$p_k(\omega) = G_k(\omega) \sum_{n \geq 1} \int dt_1 e^{i\omega t_1} g_k^{(n)*} m^n(t_1) \quad (9)$$

contain all the harmonics of coherent magnon amplitude, where the phonon's Green function $G_k(\omega) = 1/(\omega - \omega_k + i\delta_p)$.

The magnon amplitude, on the other hand, should be self-consistently solved by the nonlinear equation, to the leading two orders of the coupling constants,

$$\begin{aligned} m(\omega) &= \frac{1}{\omega - \omega_F + i\delta_m} \left[\sum_k G_k(\omega) |g_k^{(1)}|^2 m(\omega) \right. \\ &\quad + 6 \sum_{k, \omega_1, \omega_2} G_k(\omega + \omega_1) |g_k^{(2)}|^2 m^*(\omega_2) m(\omega_1) m(\omega + \omega_2 - \omega_1) \\ &\quad \left. - i\mu_0 \sqrt{\gamma M_s V / (2\hbar)} \xi_m h_{x'}(\omega) \right]. \end{aligned} \quad (10)$$

Treating the phonon's back action to the FMR as a perturbation, here we pursue an iteration solution of Eq. (10). Substituting the unperturbed solution $m^{(0)}(\omega) \approx -i\mu_0 \sqrt{\gamma M_s V / 2\hbar} \xi_m h_{x'}(\omega) / (\omega - \omega_F + i\delta_m)$ into (10), we arrive at

$$m(\omega) \approx \frac{-i\mu_0 \sqrt{\gamma M_s V / (2\hbar)} \xi_m h_{x'}(\omega)}{\omega - \omega_F + i\delta_m + \Sigma_L(\omega) + \Sigma_{NL}(\omega)}, \quad (11)$$

where $\Sigma_L(\omega) = -\sum_k G_k(\omega) |g_k^{(1)}|^2$ and $\Sigma_{NL}(\omega) = -6ln_m \sum_k G_k(\omega + \omega_F) |g_k^{(2)}|^2$ are self energies contributed, respectively, by the linear and nonlinear phonon pumping. $n_m \equiv \langle \hat{m}^\dagger(t) \hat{m}(t) \rangle =$

$[\mu_0 \sqrt{\gamma M_s w d / (2\hbar)} \xi_m h_{x'}(\omega_F)]^2$ is the pumped magnon number per unit wire length. Around FMR, the imaginary part of Σ , i.e., $\text{Im} \Sigma_L(\omega_F) = L / (2c_r) (|g_{-k_r}^{(1)}|^2 + |g_{k_r}^{(1)}|^2)$ and $\text{Im} \Sigma_{NL}(\omega_F) = 3Lln_m / c_r (|g_{-2k_r}^{(2)}|^2 + |g_{2k_r}^{(2)}|^2)$ contribute to linear and nonlinear magnon dampings, where L is the substrate's length and $k_r = \omega_F / c_r$.

Substituting the solutions $p_k(t)$ (9) and $m(t)$ (11) to the displacement field (7), we close the momentum integral in the upper (lower) half complex plane when $x > 0$ ($x < 0$). When $x > 0$, the displacement field

$$\mathbf{u}_R = \frac{2L}{c_r} \sum_{n \geq 1} \text{Im} \left(\mathbf{u}(z, nk_r) e^{ink_r x} g_{nk_r}^{(n)*} m^n(t) \right), \quad (12)$$

only appears on the right-hand side of the nanowire but on its left-hand side

$$\mathbf{u}_L = \frac{2L}{c_r} \sum_{n \geq 1} \text{Im} \left(\mathbf{u}(z, -nk_r) e^{-ink_r x} g_{-nk_r}^{(n)*} m^n(t) \right). \quad (13)$$

Solutions (12) and (13) contain both the linear and nonlinear phonon pumping effects. $|\mathbf{u}_L| \neq |\mathbf{u}_R|$ with the non-reciprocal couplings.

With the parameters in the simulation, solutions (12) and (13) reproduce the numerical results well with $m(t) \rightarrow \sqrt{ldw / (2\gamma\hbar M_s)} (iM_{x'}(t) / \xi_m - \xi_m M_{z'}(t))$, calculated from Eq. (11) by disregarding the small damping, and proper coupling constants, as shown in Fig. 3. Our quantum formalism is thereby established for the future study of quantum communication with on-chip magnons [60–62] mediated by high-quantity acoustic oscillation.

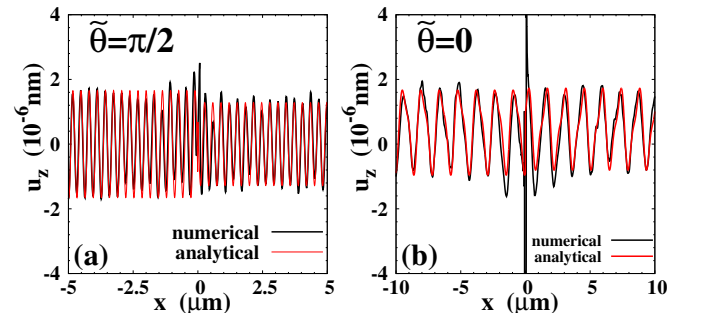


Figure 3. Calculated SHG and linear phonon pumping by analytical solutions (12) and (13) with the simulation parameters. We use $g_{2k_r}^{(2)} = 0.76$ mHz and $g_{-2k_r}^{(2)} = 0.98$ mHz in (a), and $g_{k_r}^{(1)} = 1.2$ kHz, $g_{-k_r}^{(1)} = 1.3$ kHz, $g_{2k_r}^{(2)} = 0.21$ mHz, and $g_{-2k_r}^{(2)} = 0.2$ mHz in (b).

Directional SHG by magnetic nano-disc.—It is convenient to resolve the above direction-dependent phonon pumping by a magnetic nano-disc. We consider a YIG disk of thickness $d = 80$ nm and radius $r = 150$ nm on the GGG substrate, with the magnetization biased along the $\hat{\mathbf{y}}$ -direction by a static magnetic field $\mu_0 H_0 = 0.1$ T. The

demagnetization factor $N_{xx} = N_{yy} \simeq d/(2d + \sqrt{\pi}r)$, and $N_{zz} \simeq \sqrt{\pi}r/(2d + \sqrt{\pi}r)$ [63]. We apply a similar magnetic field pulse centered at frequency $\omega_F = 4$ GHz to the wire case such that the excited transverse magnetization $M_z = 0.15M_s$. Figure 4 shows the pumped displacement fields u_z and u_x at the surface $z = 0$ of the substrate. There exists a special direction denoted by the dashed line that exhibits pure SHG without any linear and third harmonics when the pumped SAWs propagate normally to \mathbf{M}_s direction, similar to that by the magnetic wires. The SHG mixes with the linear phonon pumping, however, when the SAWs propagate in the other directions.

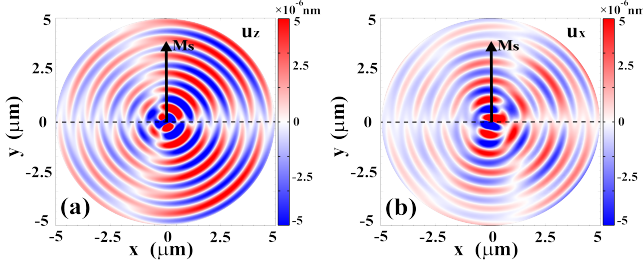


Figure 4. Pumped displacement fields u_z [(a)] and u_x [(b)] at the surface $z = 0$ of GGG substrate by the FMR of YIG disc of thickness $d = 80$ nm and radius $r = 150$ nm, which is saturated along the \hat{y} -direction. The dashed line indicates the pattern with pure SHG.

Conclusion.—In conclusion, we predict the acoustic frequency comb with frequency multiplication of SAWs by magnetic transducers when driven by microwaves. We further predict the conditions to realize the pure acoustic SHG without any linear and third harmonics, a functionality beyond those by anharmonic interaction of lattice [28–31]. Such a magnetic approach may overcome the difficulty in the electric technique in coherent phonon generation since it allows high-frequency (> 10 GHz) excitation of phonons by microwaves with ultra low energy consumption and unprecedented tunability with different magnetic configurations and material choices, thus particularly useful in miniaturized phononic, magnonic, and spintronic devices.

This work is financially supported by the National Natural Science Foundation of China under Grant No. 0214012051, and the startup grant of Huazhong University of Science and Technology (Grants No. 3004012185 and No. 3004012198). W.Y. is supported by National Natural Science Foundation of China under Grant No. 12204107, and Shanghai Science and Technology Committee (Grants No. 21PJ1401500 and No. 21JC1406200).

* These authors contribute equally to this work.

† taoyuphy@hust.edu.cn

- [1] E. A. Ash, A. A. Oliner, G. W. Farnell, H. M. Gerard, A. J. Slobodnik, and H. I. Smith, in *Acoustic Surface Waves* (Topics in Applied Physics) (Springer, Berlin, 2014).
- [2] G. S. Kino, *Acoustic Waves: Devices, Imaging, and Analog Signal Processing* (Prentice-Hall, New Jersey, 1987).
- [3] M. V. Gustafsson, T. Aref, A. F. Kockum, M. K. Ekstrom, G. Johansson, and P. Delsing, Propagating phonons coupled to an artificial atom, *Science* **346**, 207 (2014).
- [4] M. J. A. Schuetz, E. M. Kessler, G. Giedke, L. M. K. Vandersypen, M. D. Lukin, and J. I. Cirac, Universal Quantum Transducers Based on Surface Acoustic Waves, *Phys. Rev. X* **5**, 031031 (2015).
- [5] K. J. Satzinger, Y. P. Zhong, H.-S. Chang, G. A. Peairs, A. Bienfait, M.-H. Chou *et al.*, Quantum control of surface acoustic-wave phonons, *Nature (London)* **563**, 661 (2018).
- [6] E. Dieulesaint and D. Royer, *Elastic Waves in Solids II: Generation, Acousto-Optic Interaction, Applications* (Springer, New York, 2000).
- [7] P. Delsing *et al.*, The 2019 surface acoustic waves roadmap, *J. Phys. D: Appl. Phys.* **52**, 353001 (2019).
- [8] Y. Cang, Y. Jin, B. Djafari-Rouhani, and G. Fytas, Fundamentals, progress and perspectives on high-frequency phononic crystals, *J. Phys. D: Appl. Phys.* **55**, 193002 (2022).
- [9] E. G. Spencer, R. T. Denton, and R. P. Chambers, Temperature dependence of microwave acoustic losses in yttrium iron garnet, *Phys. Rev.* **125**, 1950 (1962).
- [10] M. Dutoit, Microwave phonon attenuation in yttrium aluminum garnet and gadolinium gallium garnet, *J. Appl. Phys.* **45**, 2836 (1974).
- [11] S. Streib, H. Keshtgar, and G. E. W. Bauer, Damping of magnetization dynamics by phonon pumping, *Phys. Rev. Lett.* **121**, 027202 (2018).
- [12] O. S. Latcham, Y. I. Gusieva, A. V. Shytov, O. Y. Gorobets, and V. V. Kruglyak, Controlling acoustic waves using magneto-elastic Fano resonances, *Appl. Phys. Lett.* **115**, 082403 (2019).
- [13] K. An, A. N. Litvinenko, R. Kohno, A. A. Fuad, V. V. Naletov, L. Vila, U. Ebels, G. de Loubens, H. Hurdequint, N. Beaulieu, J. B. Youssef, N. Vukadinovic, G. E. W. Bauer, A. N. Slavin, V. S. Tiberkevich, and O. Klein, Coherent long-range transfer of angular momentum between magnon Kittel modes by phonons, *Phys. Rev. B* **101**, 060407 (2020).
- [14] A. Rückriegel and R. A. Duine, Long-range phonon spin transport in ferromagnet-nonmagnetic insulator heterostructures, *Phys. Rev. Lett.* **124**, 117201 (2020).
- [15] X. Zhang, G. E. W. Bauer, and T. Yu, Unidirectional pumping of phonons by magnetization dynamics, *Phys. Rev. Lett.* **125**, 077203 (2020).
- [16] T. Yu, Nonreciprocal surface magnetoelastic dynamics, *Phys. Rev. B* **102**, 134417 (2020).
- [17] K. Yamamoto, W. Yu, T. Yu, J. Puebla, M. Xu, S. Maekawa, and G. E. W. Bauer, Non-reciprocal pumping of surface acoustic waves by spin wave resonance, *J. Phys. Soc. Jpn.* **89**, 113702 (2020).
- [18] K. An, R. Kohno, A. N. Litvinenko, R. L. Seeger, V. V. Naletov, L. Vila, G. de Loubens, J. Ben Youssef, N. Vukadinovic, G. E. W. Bauer, A. N. Slavin, V. S. Tiberkevich, and O. Klein, Bright and dark states of two distant macrospins strongly coupled by phonons, *Phys. Rev. X* **12**, 011060 (2022).

- [19] T. Yu, Z. C. Luo, and G. E. W. Bauer, Chirality as Generalized Spin-Orbit Interaction in Spintronics, arXiv:2206.05535.
- [20] M. F. Lewis and E. Patterson, Acoustic-Surface-Wave Isolator, Appl. Phys. Lett. **20**, 276 (1972).
- [21] M. Weiler, L. Dreher, C. Heeg, H. Huebl, R. Gross, M. S. Brandt, and S. T. B. Goennenwein, Elastically Driven Ferromagnetic Resonance in Nickel Thin Films, Phys. Rev. Lett. **106**, 117601 (2011).
- [22] M. Weiler, H. Huebl, F. S. Goerg, F. D. Czeschka, R. Gross, and S. T. B. Goennenwein, Spin Pumping with Coherent Elastic Waves, Phys. Rev. Lett. **108**, 176601 (2012).
- [23] R. Sasaki, Y. Nii, Y. Iguchi, and Y. Onose, Nonreciprocal propagation of surface acoustic wave in Ni/LiNbO₃, Phys. Rev. B **95**, 020407(R) (2017).
- [24] M. R. Xu, K. Yamamoto, J. Puebla, K. Baumgaertl, B. Rana, K. Miura, H. Takahashi, D. Grundler, S. Maekawa, and Y. Otani, Nonreciprocal surface acoustic wave propagation via magneto-rotation coupling, Sci. Adv. **6**, abb1724 (2020).
- [25] M. Küß, M. Heigl, L. Flacke, A. Hörner, M. Weiler, M. Albrecht, and A. Wixforth, Nonreciprocal Dzyaloshinskii–Moriya Magnetoacoustic Waves, Phys. Rev. Lett. **125**, 217203 (2020).
- [26] P. J. Shah, D. A. Bas, I. Lisenkov, A. Matyushov, N. Sun, and M. R. Page, Giant nonreciprocity of surface acoustic waves enabled by the magnetoelastic interaction, Sci. Adv. **6**, eabc5648 (2020).
- [27] R. Sasaki, Y. Nii, and Y. Onose, Magnetization control by angular momentum transfer from surface acoustic wave to ferromagnetic spin moments, Nat. Commun. **12**, 2599 (2021).
- [28] M. Först, C. Manzoni, S. Kaiser, Y. Tomioka, Y. Tokura, R. Merlin, and A. Cavalleri, Nonlinear phononics as an ultrafast route to lattice control, Nat. Phys. **7**, 854 (2011).
- [29] A. Bojahr, M. Gohlke, W. Leitenberger, J. Pudell, M. Reinhardt, A. von Reppert, M. Roessle, M. Sander, P. Gaal, and M. Bargheer, Second Harmonic Generation of Nanoscale Phonon Wave Packets, Phys. Rev. Lett. **115**, 195502 (2015).
- [30] A. Ganesan, C. Do, and A. Seshia, Phononic Frequency Comb via Intrinsic Three-Wave Mixing, Phys. Rev. Lett. **118**, 033903 (2017).
- [31] L. Shao, D. Zhu, M. Colangelo, D. Lee, N. Sinclair, Y. Hu, P. T. Rakich, K. Lai, K. K. Berggren, and M. Lončar, Electrical control of surface acoustic waves, Nat. Electron. **5**, 348 (2022).
- [32] A. Barman *et al.*, The 2021 Magnonics Roadmap, J. Phys.: Condens. Matter **33**, 413001 (2021).
- [33] A. Brataas, B. van Wees, O. Klein, G. de Loubens, and M. Viret, Spin insulatronics, Phys. Rep. **885**, 1 (2020).
- [34] C. Koerner, R. Dreyer, M. Wagener, N. Liebing, H. G. Bauer, and G. Woltersdorf, Frequency multiplication by collective nanoscale spin-wave dynamics, Science **375**, 1165 (2022).
- [35] T. Hula, K. Schultheiss, F. J. T. Goncalves, L. Körber, M. Bejarano, M. Copus, L. Flacke, L. Liensberger, A. Buzdakov, A. Kákay, M. Weiler, R. Camley, J. Fassbender, and H. Schultheiss, Spin-wave frequency combs, Appl. Phys. Lett. **121**, 112404 (2022).
- [36] J. W. Rao, B. M. Yao, C. Y. Wang, C. Zhang, T. Yu, and W. Lu, Unveiling Pump induced Magnon Mode via its Strong Interaction with Walker Modes, arXiv:2204.04590.
- [37] J. J. Carmiggelt, I. Bertelli, R. W. Mulder, A. Teepe, M. Elyasi, B. G. Simon, G. E. W. Bauer, Y. M. Blanter, and T. van der Sar, Broadband microwave detection using electron spins in a hybrid diamond-magnet sensor chip, arXiv:2206.07013.
- [38] C. Kittel, Interaction of Spin Waves and Ultrasonic Waves in Ferromagnetic Crystals, Phys. Rev. **110**, 836 (1958).
- [39] Z. Tian, D. Sander, and J. Kirschner, Nonlinear magnetoelastic coupling of epitaxial layers of Fe, Co, and Ni on Ir(100), Phys. Rev. B **79**, 024432 (2009).
- [40] T. L. Gilbert, A phenomenological theory of damping in ferromagnetic materials, IEEE Trans. Magn. **40**, 3443 (2004).
- [41] L. D. Landau and E. M. Lifshitz, *Electrodynamics of Continuous Media*, 2nd ed. (Butterworth-Heinemann, Oxford, 1984).
- [42] T. Yu, H. C. Wang, M. A. Sentef, H. M. Yu, and G. E. W. Bauer, Magnon trap by chiral spin pumping, Phys. Rev. B **102**, 054429 (2020).
- [43] T. Sato, W. C. Yu, S. Streib, and G. E. W. Bauer, Dynamic magnetoelastic boundary conditions and the pumping of phonons, Phys. Rev. B **104**, 014403 (2021).
- [44] S. P. Timoshenko and J. N. Goodier, *Theory of Elasticity*, (McGraw-Hill, New York, 1970).
- [45] L. D. Landau and E. M. Lifshitz, *Theory of Elasticity*, (Pergamon Press, Oxford, New York, Toronto, Sydney, Paris, Braunschweig, 1970).
- [46] See Supplementary Material at [...] for the detailed derivations of the magnetic equilibrium configurations, magnon Hamiltonian, magnon-phonon coupling Hamiltonian, and nonlinear phonon pumping.
- [47] COMSOL Multiphysics®, <http://www.comsol.com>.
- [48] W. C. Yu, Micromagnetic Simulation with COMSOL Multiphysics, <https://www.comsol.com/blogs/micromagnetic-simulation-with-comsol-multiphysics/>.
- [49] Q. Wang, B. Heinz, R. Verba, M. Kewenig, P. Pirro, M. Schneider, T. Meyer, B. Lägél, C. Dubs, T. Brächer, and A. V. Chumak, Spin Pinning and Spin-Wave Dispersion in Nanoscopic Ferromagnetic Waveguides, Phys. Rev. Lett. **122**, 247202 (2019).
- [50] M. Schreier, A. Kamra, M. Weiler, J. Xiao, G. E. W. Bauer, R. Gross, and S. T. B. Goennenwein, Magnon, phonon, and electron temperature profiles and the spin Seebeck effect in magnetic insulator/normal metal hybrid structures, Phys. Rev. B **88**, 094410 (2013).
- [51] I. A. Viktorov, *Rayleigh and Lamb waves: Physical theory and applications* (Plenum Press, New York, 1967).
- [52] C. Kittel, *Quantum Theory of Solids* (Wiley, New York, 1963).
- [53] T. Holstein and H. Primakoff, Field Dependence of the Intrinsic Domain Magnetization of a Ferromagnet, Phys. Rev. **58**, 1098 (1940).
- [54] L. R. Walker, Magnetostatic Modes in Ferromagnetic Resonance, Phys. Rev. **105**, 390 (1957).
- [55] R. Verba, G. Melkov, V. Tiberkevich, and A. Slavin, Collective spin-wave excitations in a two-dimensional array of coupled magnetic nanodots, Phys. Rev. B **85**, 014427 (2012).
- [56] S. Sharma, Y. M. Blanter, and G. E. W. Bauer, Light scattering by magnons in whispering gallery mode cavities, Phys. Rev. B **96**, 094412 (2017).

- [57] T. Yu, S. Sharma, Y. M. Blanter, and G. E. W. Bauer, Surface dynamics of rough magnetic films, *Phys. Rev. B* **99**, 174402 (2019).
- [58] C. W. Gardiner and M. J. Collett, Input and output in damped quantum systems: Quantum stochastic differential equations and the master equation, *Phys. Rev.* **31**, 3761 (1985).
- [59] A. A. Clerk, M. H. Devoret, S. M. Girvin, F. Marquardt, and R. J. Schoelkopf, Introduction to quantum noise, measurement, and amplification, *Rev. Mod. Phys.* **82**, 1155 (2010).
- [60] J. Zou, S. Zhang, and Y. Tserkovnyak, Bell-state generation for spin qubits via dissipative coupling, *Phys. Rev. B* **106**, L180406 (2022).
- [61] M. Fukami, D. R. Candido, D. D. Awschalom, and M. E. Flatté, Opportunities for Long-Range Magnon-Mediated Entanglement of Spin Qubits via On- and Off-Resonant Coupling, *PRX Quantum* **2**, 040314 (2021).
- [62] B. W. Zeng and T. Yu, Radiation-free and non-Hermitian topology inertial defect states of on-chip magnons, [arXiv:2209.13386](https://arxiv.org/abs/2209.13386).
- [63] M. Sato, Simple and approximate expressions of demagnetizing factors of uniformly magnetized rectangular rod and cylinder, *J. Appl. Phys.* **66**, 983 (1989).